Effective Resistance and Leakage Inductance in Multiwinding Transformers: Modeling, Measurement and Comparison with Numerical Solution

Adalberto J. Batista
U. F. de Goiás/EEE
74605-220
Goiânia, GO - Brasil
batista@eee.ufg.br

João C. S. Fagundes
U. F. de Santa Catarina/INEP
88040-970
Florianópolis, SC - Brasil
fagundes@inep.ufsc.br

Philippe Viarouge
Université Laval/LEEPCI
G1K 7P4
Québec, PQ - Canada
viarouge@gel.ulaval.ca

Jérôme Cros
Université Laval/LEEPCI
G1K 7P4
Québec, PQ - Canada
cros@gel.ulaval.ca

***Abstract* - Skin and proximity effects are significant factors to consider when calculating effective resistances and leakage inductances in transformers, specially for those used in high frequency power conversion. This paper presents generalized expressions to calculate these effective parameters for multiwinding transformers obtained through one- and two-dimensional analytically based approaches. Experimental data and electromagnetic field computation based data are provided for comparison and validation purposes.**

I. Introduction

The design of compact and efficient magnetic components for high frequency power conversion applications, such as transformers and inductors for switched mode power supplies, requires accurate models of core and winding losses. Considerable mathematical modeling efforts carried out over the past few years have resulted in one- and two-dimensional models to predict winding losses [1,2] in such components. The one-dimensional model proposed by Vandelac and Ziogas [1] assumes that the three-dimensional magnetic field in the component winding space varies in only one dimension, is uniformly distributed and ignores the effect of winding curvature. This model can be used to predict winding losses in magnetic components with multilayer windings of foil conductors under arbitrary periodic current excitation. In the case of windings with solid round wire or litz wire, this model requires the replacement of the actual winding layers by equivalent-foil conductors as in the original model. The two-dimensional model proposed by Ferreira [2], which also ignores the effect of winding curvature, is based on the orthogonality that exists between the spatial current distributions due to skin and proximity effects in symmetrical conductors immersed in an external magnetic field that is perpendicular to their axes. It allows, for an arbitrary periodic current excitation, the calculation of losses due to skin and proximity effects separately and takes the actual conductor's geometrical shape into account, but a detailed knowledge of the magnetic field distribution across the winding section is required to calculate the proximity effect losses. In order to obtain an analytical solution to this problem, as required by the design optimization procedure of the component [3], it must be assumed that this field distribution is one-dimensional and uniform in the conductor cross-section.

Although receiving considerably less attention and often ignored, the time-average magnetic energy stored in the winding magnetic field can be just as important, significantly affecting circuit operation at high frequencies. Niemela et al [4] have proposed a method to calculate this energy, which is based upon Vandelac and Ziogas's work.

This paper builds on the one-dimensional model proposed by Vandelac and Ziogas [1], hereinafter referred to as thin layer model. Extending its pattern to the two-dimensional model proposed by Ferreira [2], hereinafter referred to as orthogonality model, generalized expressions are derived for the effective resistance of multilayer windings of either solid round wire, or litz wire, or foil conductors. Similar generalized expressions for the effective resistance and leakage inductance are also obtained through the thin layer model itself, giving a unified sense to these models. An extensive work carried out by the authors, concerning the effect of winding curvature on its effective parameters, supports the conditions under which these expressions will be theoretically valid [3]. To the authors' knowledge, these solutions, when applied to transformers with multilayer windings under non-sinusoidal current excitation, usually the practical case, have not been reported in previous works. In addition, experimental data are provided to illustrate the accuracy and the limitations of such mathematical modeling.

The limitations of these models, e.g. when the conductors are subject to end-effect losses due to radial magnetic fields, can be studied by using a numerical technique such as the finite element method (FEM) and the finite difference method (FDM). In this paper, these limitations are studied by using Difimédi [5], a two-dimensional FDM software package. For comparison between theoretical and experimental results, an automated system for winding loss measurement was implemented.

II. Mathematical Modeling

A. Thin Layer Model

In the one-dimensional case, the magnetic field in the winding space is assumed to be parallel to the center leg of the core. It is reasonable to expect that, with a high permeability pot core surrounding the winding structure, such a field pattern will be produced, and experimental results indicate that the assumption of parallel field lines is also a valid one for high permeability cores of different geometry, such as EE, EC, and RM cores. In addition, it is assumed that the winding structure is axisymmetric and constituted of foil conductors, which span the entire breadth of the core window. Finally, the currents in the

layers are assumed to have identical waveforms. Under these assumptions, the general solutions to the magnetic field and current density within the n'th conducting layer of a winding can be obtained in cylindrical coordinates from Maxwell's equations. The particular solutions to these electromagnetic quantities can be determined by applying the boundary conditions of magnetic field phasor at the innermost and the outermost surfaces of the layer. Once these solutions are obtained, the solutions to the power dissipation and the magnetic energy storage within the n'th conducting layer can be obtained from Poynting's theorem. The solutions to the power dissipation and the magnetic energy storage in the multilayer winding can be obtained by adding the results obtained for each layer in particular. In this sum the magnetic energy stored in the insulation layers of the winding must be taken into account. Finally, according to Fourier's analysis, these solutions can be extended to non-sinusoidal periodic current excitation by adding the results obtained for dc excitation and for all harmonic components of the current waveform.

The detailed one-dimensional mathematical modeling of power dissipation and magnetic energy storage in a multilayer winding of a multiwinding magnetic component, an analysis of design optimization techniques and graphical displays concerning, among others, the effect of curvature on these quantities, are contained in [3].

Fig. 1 shows a cross-section of a multiwinding magnetic component where the structure of a particular multilayer winding is detailed. If the conductor layer thickness is h, the mean layer radius is r_n, and the mean winding radius is r_w, then the conditions under which the effect of curvature can be ignored are given by (1) and (2) [3]:

$$r_n \geq 4h \tag{1}$$

$$r_w \cong r_n \tag{2}$$

The particular one-dimensional model obtained under these conditions is named thin layer model. According to derivations in [3], based on this model, the expressions for calculating the effective resistance, R_e, and the effective leakage inductance, L_e, of multilayer windings of foil

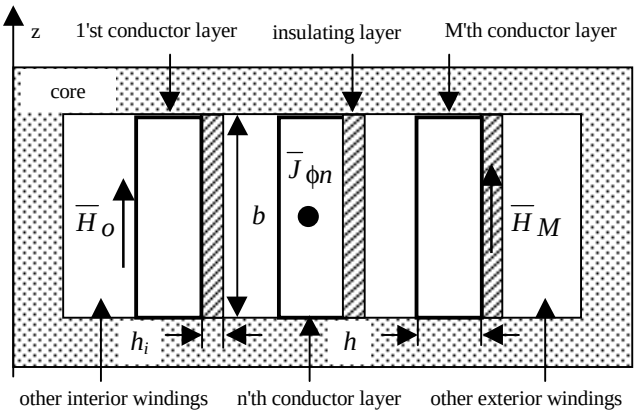

Figure 1. Cross-sectional view of a multiwinding magnetic component.

conductors, under non-sinusoidal periodic current excitation, are given by (3) and (4), respectively:

$$\frac{R_e}{R_{dc}} = \left[\frac{I_{dc}}{I_{ef}}\right]^2 + \frac{1}{3}\sum_{j=1}^{\infty}\left[\frac{I_{efj}}{I_{ef}}\right]^2 \frac{\underline{h}_j}{\left|1-\overline{\varphi}_j\right|^2}\{ F_1(\underline{h}_j)[(2M^2+1)(1+\left|\overline{\varphi}_j\right|^2)+2(M^2-1)\Re(\overline{\varphi}_j)] + -4F_2(\underline{h}_j)[(M^2-1)(1+\left|\overline{\varphi}_j\right|^2)+(M^2+2)\Re(\overline{\varphi}_j)]\} \tag{3}$$

$$\frac{\omega L_e}{R_{dc}} = \frac{\underline{h}_1}{3}\left[\frac{I_{dc}}{I_{ef}}\right]^2 \frac{1}{\left|1-\varphi_{cc}\right|^2}\{ \underline{h}_{i1}[(2M^2+1)(1+\varphi_{cc}^2)+2(M^2-1)\varphi_{cc} + 3M(1-\varphi_{cc}^2)] + 2\underline{h}_1 M^2[1+\varphi_{cc}+\varphi_{cc}^2]\} + \frac{\underline{h}_1}{3}\sum_{j=1}^{\infty}\left[\frac{I_{efj}}{I_{ef}}\right]^2 \frac{1}{\left|1-\overline{\varphi}_j\right|^2}\frac{1}{\sqrt{j}}\{ \underline{h}_{ij}[(2M^2+1)(1+\left|\overline{\varphi}_j\right|^2)+ 2(M^2-1)\Re(\overline{\varphi}_j)+3M(1-\left|\overline{\varphi}_j\right|^2)] + F_3(\underline{h}_j)[(2M^2+1)(1+\left|\overline{\varphi}_j\right|^2)+2(M^2-1)\Re(\overline{\varphi}_j)] + -4F_4(\underline{h}_j)[(M^2-1)(1+\left|\overline{\varphi}_j\right|^2)+(M^2+2)\Re(\overline{\varphi}_j)]\} \tag{4}$$

where:

$$F_{1,3}(\underline{h}_j) = \frac{senh(2\underline{h}_j) \pm sen(2\underline{h}_j)}{cosh(2\underline{h}_j) - cos(2\underline{h}_j)} \tag{5}$$

$$F_{2,4}(\underline{h}_j) = \frac{senh(\underline{h}_j)cos(\underline{h}_j) \pm cosh(\underline{h}_j)sen(\underline{h}_j)}{cosh(2\underline{h}_j) - cos(2\underline{h}_j)} \tag{6}$$

$$\underline{h}_j = h/\delta_j \tag{7}$$

$$\underline{h}_{ij} = h_i/\delta_j \tag{8}$$

$$\delta_j = \sqrt{2/j\omega\mu_o\sigma_c} \tag{9}$$

$$\overline{\varphi} = \overline{H}_o/\overline{H}_M \tag{10}$$

In the above equations, R_{dc} is the dc resistance of the winding, I_{dc} is the dc component of the current waveform, I_{ef} is the rms value of this waveform, I_{efj} is the rms value of its j'th harmonic component, ω is the fundamental angular frequency, σ_c is the copper conductivity and μ_o is the free space permeability.

To permit calculating the winding boundary-condition

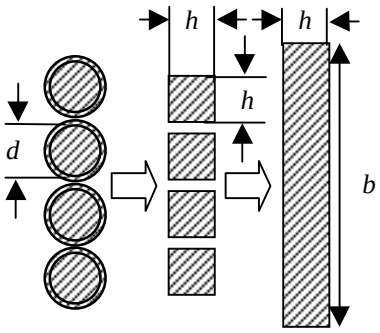

Figure 2. Steps in transforming a layer of solid round wire into an equivalent layer of foil conductor.

ratio, defined by (10), the frequency-independent magnetic field phasors between windings, caused by the dc component and by each harmonic component of their current waveforms, must be determined.

For windings of solid round wire or litz wire, the actual winding layers can be approximated by equivalent layers of foil conductor, which span the entire breadth of the core window as illustrated in Fig. 2 [1]. In this figure, the round conductors are replaced by square conductors of equal conducting cross-sectional area, which are brought together into a single layer foil, then stretched in order to fill the entire window breadth without changing the height of the layer. To compensate the increase in the cross-sectional area of the conducting layer, an effective conductivity $\eta\sigma_C$ is used in the field equations for the layer. The layer porosity, η, is defined as $\eta = N_b h/b$, where N_b is the number of conductor cross-sections appearing in a cross-sectional view of the winding layer, and b is the core window breadth. Layers of litz wire are transformed similarly [3]. First, it is assumed that the total current is divided evenly among the individual strands. Second, the bunch of N_s strands with diameter d_S is replaced by a squared arrangement of $\sqrt{N_s}$ x $\sqrt{N_s}$ conductors of equal diameter. The resultant $\sqrt{N_s}$ layers of round wire are then transformed as described previously. Therefore, for layers of litz wire, whose overall diameter is D_l, N_b is given by $N_l\sqrt{N_s}$, where N_l is the number of turns per layer.

B. Orthogonality Model

The current density vector phasor in a conductor, $\bar{\mathbf{J}}$, can be expressed as the sum of the current density vector phasor due to skin effect, $\bar{\mathbf{J}}_s$, and the current density vector phasor due to proximity effect, $\bar{\mathbf{J}}_p$. Then, under the condition of orthogonality between skin and proximity effects, expressed by (11), the power losses in the conductor, in watts per meter, can be expressed as the sum of the power losses due to skin effect, P_s, given by (12), and the power losses due to proximity effect, P_p, given by (13).

$$\iint_S (\bar{J}_{\phi s}\bar{J}_{\phi p}^{*})ds = \iint_S (\bar{J}_{\phi s}^{*}\bar{J}_{\phi p})ds = 0 \tag{11}$$

$$P_s = \frac{1}{2\sigma_c}\iint_S \left|\bar{J}_{\phi s}\right|^2 ds \tag{12}$$

$$P_p = \frac{1}{2\sigma_c}\iint_S \left|\bar{J}_{\phi p}\right|^2 ds \tag{13}$$

According to derivations in [3], based on the orthogonality model, under the assumption that the field distribution in the winding space is one-dimensional and, in addition, is uniform in the conductor cross-section, the expressions for the ratio between effective resistance and dc resistance of multilayer windings of foil conductors, solid round wire, and litz wire under non-sinusoidal current excitation, are given by (14), (15) and (16), respectively:

$$\frac{R_{ef}}{R_{dcf}} = \left[\frac{I_{dc}}{I_{ef}}\right]^2 + \sum_{j=1}^{\infty}\left[\frac{I_{efj}}{I_{ef}}\right]^2 \frac{\underline{h}_j}{2}\{ [F_1(\underline{h}_j) + 2F_2(\underline{h}_j)] + \frac{1}{3}\Gamma(M,\bar{\varphi}_j)[F_1(\underline{h}_j) - 2F_2(\underline{h}_j)]\} \tag{14}$$

$$\frac{R_{er}}{R_{dcr}} = \left[\frac{I_{dc}}{I_{ef}}\right]^2 + \sum_{j=1}^{\infty}\left[\frac{I_{efj}}{I_{ef}}\right]^2 \frac{\underline{d}_j}{2}[\Psi_1(\underline{d}_j) + \frac{\pi^2}{6}\Gamma(M,\bar{\varphi}_j)\Psi_2(\underline{d}_j)] \tag{15}$$

$$\frac{R_{el}}{R_{dcl}} = \left[\frac{I_{dc}}{I_{ef}}\right]^2 + \sum_{j=1}^{\infty}\left[\frac{I_{efj}}{I_{ef}}\right]^2 \frac{\underline{d}_{sj}}{2}\{ \Psi_1(\underline{d}_{sj}) + [1 + \frac{\pi^2}{6}\Gamma(M,\bar{\varphi}_j)]pN_s\Psi_2(\underline{d}_{sj})\} \tag{16}$$

where:

$$\Gamma(M,\bar{\varphi}_j) = 4M^2\frac{1 + \left|\bar{\varphi}_j\right|^2 + \Re(\bar{\varphi}_j)}{\left|1 - \bar{\varphi}_j\right|^2} - 1 \tag{17}$$

$$\Psi_1(\underline{d}_j) = \frac{ber_0(\underline{d}_j)bei'(\underline{d}_j) - bei_0(\underline{d}_j)ber'(\underline{d}_j)}{(ber'(\underline{d}_j))^2 + (bei'(\underline{d}_j))^2} \tag{18}$$

$$\Psi_2(\underline{d}_j) = -\frac{ber_2(\underline{d}_j)ber'(\underline{d}_j) + bei_2(\underline{d}_j)bei'(\underline{d}_j)}{(ber(\underline{d}_j))^2 + (bei(\underline{d}_j))^2} \tag{19}$$

$$\underline{d}_j = d/\sqrt{2}\delta_j \tag{20}$$

$$\underline{d}_{sj} = d_s/\sqrt{2}\delta_j \tag{21}$$

$$p = N_s d_s^2/D_l^2 \tag{22}$$

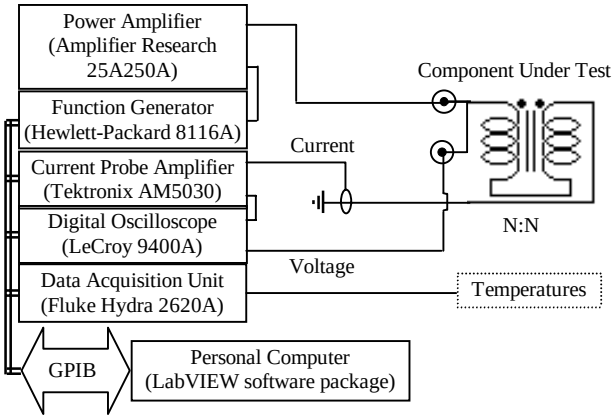

Figure 3. Automated system for winding loss measurement and validation of the developed models.

III. Measurement System

Fig. 3 presents a block diagram of the implemented system for winding loss measurement and effective parameters calculation. In this case, a power amplifier, whose bandwidth is 10 kHz to 250 MHz and maximum output power is 35 W, is used. In the case of high current and low frequency sine wave excitation, an assemblage of ac-dc and dc-ac static converters and a current transformer replaces the power amplifier. In this assemblage, the maximum frequency is 1,600 Hz and the current can be as great as 100 A. The component under test is wound as an N:N transformer, whose windings are series connected and wound in such a way that the magnetic induction in the core and, therefore, the core losses, can be neglected.

A specific software, based on the virtual instrument concept [6], was developed to perform acquisition, analysis, and presentation of the measurement data; instruments and measurement process control; and output data computation and presentation. The computer communicates with the instruments through a GPIB interface. This software requires, among other data, the frequency range, the number of frequency sweeps, data about the winding (dc resistance at ambient temperature, number of layers and turns per layer, mean turn length, insulating thickness) and its conductor. By using actual values of frequency and temperature, this software allows the computation of: a) the effective leakage inductance, using the thin layer model; b) the effective resistance, using either the thin layer or the orthogonality model; and c) the respective experimental results associated with each winding of the component under test. Furthermore, it can be applied to windings of either foil conductors, or solid round wire, or litz wire. The experimental effective parameters are obtained by using the acquired data and basic relationships of the theory of electrical circuits. These data are constituted by the terminal voltage and current of the winding and its temperature. The current waveform is sensed through a current probe or, in the case of low current, it can be determined from a voltage measurement at the terminals of a current- sensing resistor (CSR). The software includes a specific routine for this purpose, which uses a Fourier transform (fast Fourier transform or discrete Fourier transform) algorithm. This routine requires the equivalent circuit parameters of the CSR. The winding loss is obtained by computing the mean of the product between its terminal current and voltage over an integer number of acquired cycles. In order to observe the harmonic distortion of the current waveform, the implemented software presents a harmonic analysis of this waveform and its total harmonic distortion (THD).

IV. Experimental Results

In order to verify the accuracy of the developed models, tests were performed on several transformers through the described measurement system. It must be pointed out that the expressions to calculate the effective resistance of windings of foil conductors through the thin layer and the orthogonality models are, in fact, identical.

To take into account the basic assumptions of these models and to permit a fair comparison between measured values and the values computed using a two-dimensional FDM software, it would be theoretically desirable to use ungapped pot cores and windings of foil conductor to construct these transformers. However, besides the difficulty to accommodate the breakout of large foil conductors in pot cores, the low effective impedance of such windings could jeopardize the measurement accuracy. On the other hand, concerning the design optimization of the component, it is sufficient that the models accuracy be verified in a region where the windings optimization can be achieved. Therefore, it is sufficient that the relation between the equivalent-foil layer thickness and the skin depth be in the range from zero to π [3].

Fig. 4 shows a schematic representation of a component with single layer windings of copper foil conductors, which, theoretically, satisfies the referred assumptions and the limitations of the low frequency and high current measurement set up. Its core is constituted of 52 pairs of cores EE 55/55/25 with each pair ungapped and coupled side by side with another, and whose magnetic material is the 3C80 ferrite grade (Philips). Table I gives the basic data about the foil conductors, whose dimensions fill in almost all the core window area. The insulation thickness is equal to 0.1250 mm. The voltage measurement terminals were inserted next to the core, so that the effects of the effective parameters of the termination are minimized. For the current measurement a Tektronix A6303 current probe was used. The measurement process was carried out in a frequency range from 60 Hz to 1,500 Hz. The THD of the current waveform decreased from 8.0 % at 60 Hz, where its amplitude was about 95 A, to 1.5 % at 1,500 Hz, where its amplitude was about 35 A.

The results obtained for the ratio between effective resistance and dc resistance, and for the effective leakage inductance of the innermost winding are illustrated in Fig. 5. This figure shows that the results obtained by using the referred models are fairly close to those obtained by using

either the two-dimensional FDM software or the measurement system. The maximum percentage errors in the thin layer model relative to the experimental data are 6.2 % in both cases, although occurring at different frequencies. The results obtained for the ratio between effective resistance and dc resistance of the outermost winding are qualitatively similar and show a maximum percentage error of 4.5 %. However, due to the excessive noise in the voltage waveform, the results obtained for the effective leakage inductance of this winding were not considered valid.

In order to verify the accuracy of the developed models in predicting the effective resistance of windings of solid round wire, twelve transformers were built and tested, six of them with EC 35 cores and the other six with pot 4229 cores. In both cases, the magnetic material was the 3C80 ferrite grade. Each of them was built carefully, so that its two windings were practically identical, although having different number of layers and wire diameter from the others. It must be pointed out that the conditions under which the effect of curvature can be ignored are respected in all cases.

Figures 6 and 7 show the results obtained for each winding of the transformers built, respectively, with an EC 35 core and two-layer (56 turns per layer) windings, whose bare wire diameter was 0.3200 mm (28 AWG), and with a pot 4229 core and three-layer (25 turns per layer) windings, whose bare wire diameter was 0.6426 mm. The measurement process was carried out in frequency ranges from 10 kHz to 500 kHz and from 10 kHz to 140 kHz, respectively. For the current measurement a Tektronix A6302 current probe was used and the THD of the current waveform was negligible in both cases. The voltage measurement terminals, constituted of coaxial connectors, were inserted next to the core for the same reasons described before.

Figures 6(a) and 7(a) show that the results obtained for the ratio between effective resistance and dc resistance, by using the thin layer model, are fairly closed to those obtained by using the measurement system. The percentage errors relative to the experimental data are less than 10 % and 15 %, respectively. However, the results obtained through the orthogonality model show that this model leads to inaccurate predictions for the effective resistance.

Figures 6(b) and 7(b) show the results obtained for the

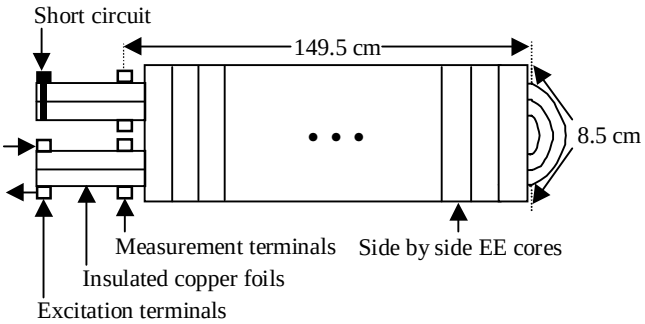

Figure 4. Schematic representation of the tested component with one-layer windings of copper foil conductors.

Table I. FOIL CONDUCTORS DATA.

Conductor	Length (m)	Width (mm)	Height (cm)	R_{dc} (mΩ)
Innermost	3.035	5.65	4.25	0.2032
Outermost	3.075	5.65	4.25	0.2059

effective leakage inductance. The analysis of these results must be conducted only from a qualitative point of view, since the thickness of the insulation layers was considered equal to zero. According to (4), the effective leakage inductance of a winding increases linearly with this thickness, independently of the frequency. Therefore, by considering the actual thickness of the insulation layers, a better agreement between the results obtained through the thin layer model and those obtained by using the measurement system would be obtained.

The results obtained for the others transformers tested are qualitatively similar. It is particularly noteworthy the resonances occurred in some cases due to the windings parasitic capacitances. The resonant frequencies, which were determined through a network analyzer (HP8753D), were suppressed by using a copper foil between the central column of the core and the innermost winding layer.

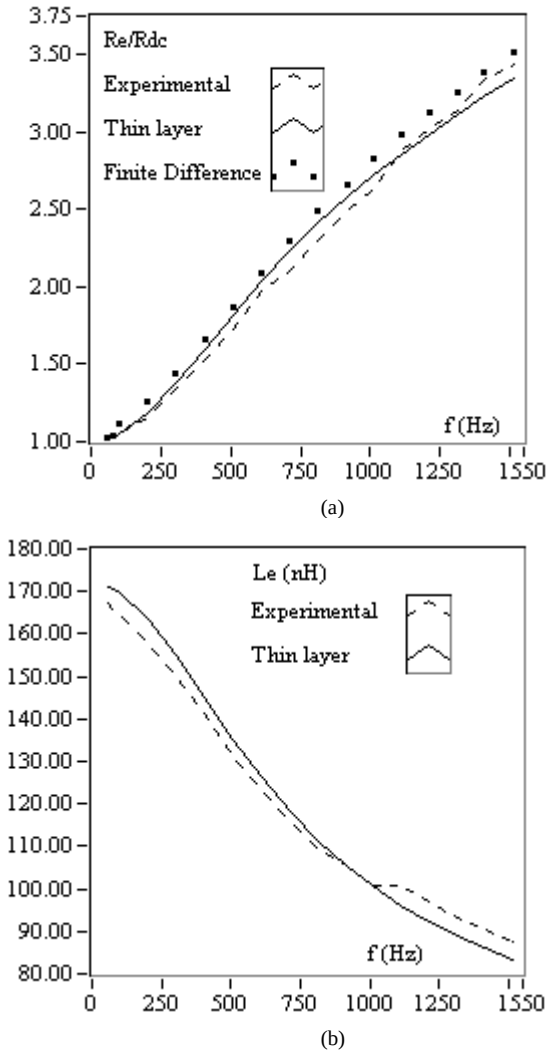

Figure 5. (a) the effective to dc resistance ratio and (b) the effective leakage inductance of the innermost winding of the structure in Fig. 4.

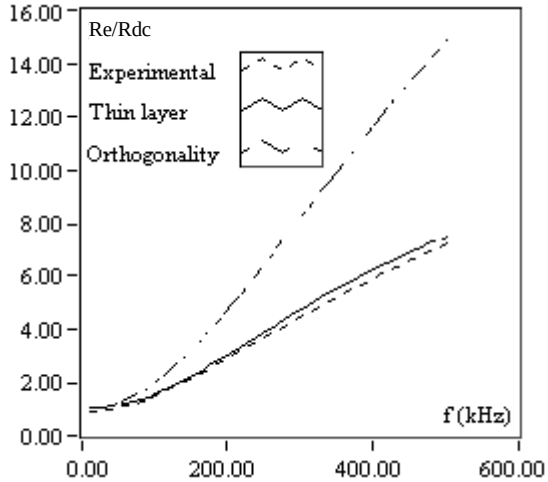

(a)

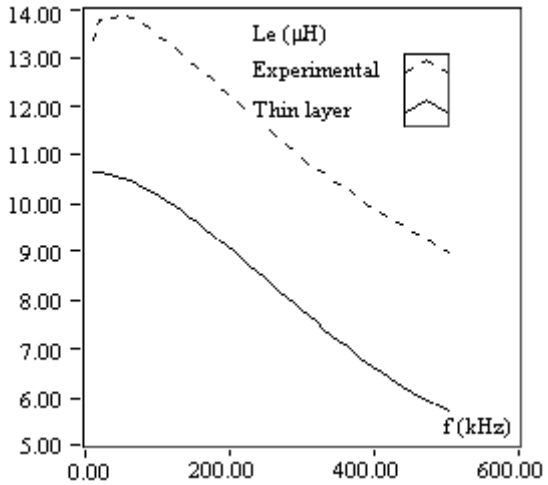

(b)

Figure 6. (a) the effective to dc resistance ratio and (b) the effective leakage inductance of each winding of the transformer built with an EC 35 core and two-layer (56 turns per layer) windings.

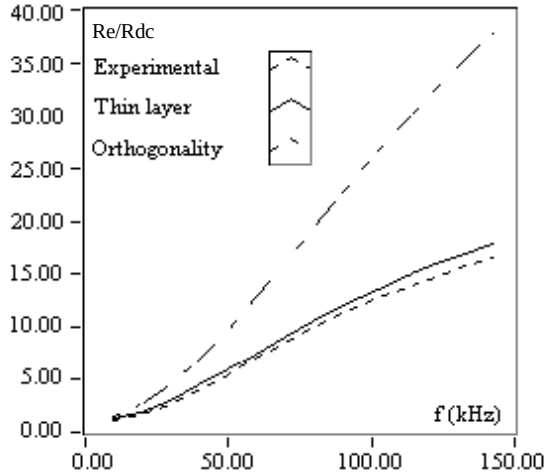

(a)

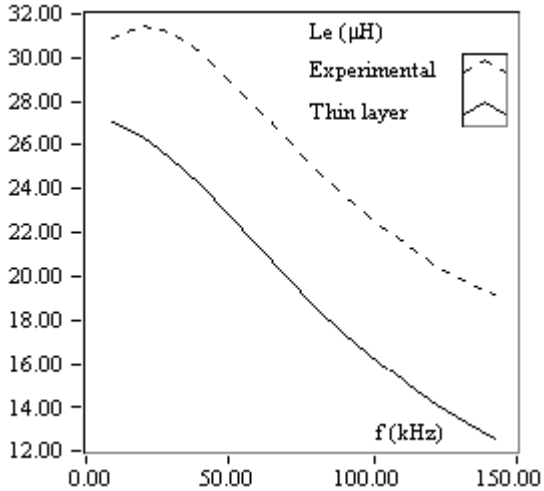

(b)

Figure 7. (a) the effective to dc resistance ratio and (b) the effective leakage inductance of each winding of the transformer built with a pot 4229 core and three-layer (25 turns per layer) windings.

V. Conclusions

In an attempt to consolidate all of the previous works in a generalized treatment, this paper introduces generalized expressions to calculate the effective resistance and the effective leakage inductance of a multilayer winding under non-sinusoidal current excitation. These expressions, obtained through the so called thin layer and orthogonality models, can be applied to windings of either solid round wire, or litz wire, or foil conductors. Experimental data, obtained for windings of either foil conductor and solid round wire, under sinusoidal current excitation, are provided, illustrating the generally good agreement between the results obtained through the thin layer model and the developed measurement system, particularly in frequency ranges where the windings optimization can be achieved. It must be pointed out that, the effective leakage inductance is greatly dependent on the insulation layers thickness, which is difficult to accurately specify for windings of either solid round wire or litz wire. The accuracy of the thin layer model in predicting the effective leakage inductance is greatly dependent on this specification.

The results obtained through the orthogonality model show that this model leads to inaccurate predictions for the effective resistance. However, the thin layer model, in spite of its simplifying assumptions, can be used as an accurate tool for design optimization purposes. The accuracy of this model in predicting the effective resistance of windings of litz wire must be verified. This will be showed in a future work.

VII. References

[1]J. P. Vandelac and P. Ziogas, "A Novel Approach for Minimizing High Frequency Transformer Copper Losses," IEEE Power Electronics Specialists Conference Record, pp. 355-367, 1987.

[2]J. A. Ferreira, "Appropriate Modeling of Conductive Losses in the Design of Magnetic Components," IEEE Power Electronics Specialists Conference Record, pp. 780-785, 1990.

[3]A. J. Batista, "Modelagem e Otimização do Projeto de Componentes Magnéticos Utilizados em Conversores Estáticos de Alta Freqüência," Tese de Doutorado, INEP, Universidade Federal de Santa Catarina, Florianópolis-SC, Brasil, 1998 (Doctoral Thesis in Portuguese).

[4]V. A. Niemela et al, "Calculating the Short-Circuit Impedances of a Multiwinding Transformer from Its Geometry," IEEE Power Electronics Specialists Conference Record, pp. 607-617, 1989.

[5]*Notice d'Utilisation de Difimédi - Code Conversationel de Calcul de Champ dans les Structures Magnétiques*, Laboratoire d'Electrotechnique et d'Electronique Industrielle, Toulouse, France, 1986.

[6]National Instruments, *LabVIEW User Manuals*, Austin, USA, 1996.